De 24/06/2026 a 27/06/2026
São Paulo
https://doi.org/10.67775/s6yjwb03

Congresso Brasileiro de Patologia das Construções

FIRE PERFORMANCE OF ADDITIVE-MODIFIED MORTARS FOR STEEL AND REINFORCED CONCRETE STRUCTURE PROTECTIONS

Fabricio L. Bolina[1]*, Débora B. Silva [2]; Eduardo C. Pachla[3]
*Autor de contato: fabriciobolina@gmail.com

[1] Departamento de Engenharia Civil, Universidade Federal do Rio Grande do Sul, Porto Alegre, Brasil
[2] Departamento de Arquitetura, Universidade Federal de Santa Maria, Santa Maria, Brasil
[3] Departamento de Estruturas e Construção Civil, Universidade Federal de Santa Maria, Santa Maria, Brasil

ABSTRACT

Building structures are vulnerable to fire, requiring design strategies that address temperature-induced mechanical degradation. This study evaluates the thermal performance of 23 mortar formulations with different compositions and additives, using experimentally derived thermal properties collected from the literature and implemented in a thermal finite element model. All mortars reduced the internal temperature of structural steel and reinforced concrete members, with effectiveness governed by coating thickness and intrinsic thermal properties. The best performance was achieved by mortars incorporating glass fiber reinforced polymer (GFRP) as a slag substitute and expanded perlite as a sand replacement, reaching temperature reductions on the order of 100%, whereas mixtures with 30% vermiculite or 15% light expanded polyvinyl chloride (PVC) as sand substitutes exhibited the lowest thermal efficiency.
Keywords: Steel structures. Reinforced concrete structures. Beams. Mortar. Fire.

RESUMO

Estruturas estão sujeitas à ação do fogo, exigindo que o projeto considere a degradação mecânica induzida por altas temperaturas. Este estudo avalia o desempenho térmico de 23 formulações de argamassas com diferentes composições e aditivos, cujas propriedades térmicas experimentais foram implementadas em um modelo numérico por elementos finitos para análise térmica. Todas as argamassas promoveram redução da temperatura interna de elementos de aço estrutural e concreto armado, com desempenho dependente da espessura do revestimento e das propriedades térmicas intrínsecas. As melhores respostas foram observadas nas argamassas com substituição de escória por polímero reforçado com fibra de vidro (GFRP) e com substituição de areia por perlita expandida, alcançando reduções de temperatura da ordem de 100%, enquanto as misturas com 30% de vermiculita ou 15% de policloreto de vinila (PVC) apresentaram o pior desempenho térmico.
Palavras-chave: Estruturas de aço. Estruturas de concreto. Vigas. Revestimentos. Fogo.

1. INTRODUCTION

Mortar coatings play a key role in enhancing the fire resistance of steel and reinforced concrete structures by acting as thermal barriers that delay heat transfer during fire. By limiting temperature rise, they help preserve structural integrity, since steel rapidly loses load-bearing capacity above 500 °C and concrete may experience cracking and spalling. In steel members, mortar layers extend the time to critical strength loss; in reinforced concrete, they help maintain the steel–concrete bond and reduce the risk of collapse. Fire-resistant mortars represent an essential passive protection strategy, with performance directly governed by their composition and thermal properties.

Rong et al. (2024) (Rong *et al.*, 2024) investigated the incorporation of glass fiber reinforced polymer (GFRP) powder as a partial binder substitute in mixtures containing cement, fly ash, and slag. Increasing GFRP content led to reductions in both thermal conductivity and density, with a more pronounced decrease in thermal conductivity. The findings indicate that GFRP enhances the thermal insulation performance of mortars, representing a strategy to improve energy efficiency without substantially affecting mass-related properties.

Topçu et al. (2024) (Topçu *et al.*, 2024) evaluated the use of sepiolite-based Phase Change Material (PCM) as a partial replacement for natural sand in mortars. The incorporation of PCM-impregnated sepiolite resulted in significant reductions in both thermal conductivity and density, indicating improved thermal insulation performance. The findings demonstrate the potential of sepiolite-based PCM systems to enhance energy efficiency in construction materials by reducing heat transfer while modifying mass-related properties.

Zhao et al. (2023) (Zhao *et al.*, 2023) investigated the feasibility of replacing natural sand with recycled carbon black (RCB) in mortars. Increasing RCB content led to progressive reductions in thermal conductivity, thermal diffusivity, and density, indicating enhanced thermal insulation capacity. These results highlight RCB as a sustainable alternative for improving the thermal performance of construction composites while promoting waste reutilization.

El Boukhari et al. (2023) (EL boukhari *et al.*, 2023) evaluated the use of olive solid waste (OSW) as a partial replacement for sand in mortar mixtures. Increasing OSW content resulted in reduced density, thermal conductivity, and thermal diffusivity, indicating improved thermal insulation performance. The findings support OSW as a sustainable alternative that enhances the thermal behavior of mortars while contributing to waste valorization in construction applications.

Adediran et al. (2023) (Adediran *et al.*, 2023) investigated the partial replacement of fayalite slag (FS) with ladle slag (LS) and blast furnace slag (BFS) in FS-based mortars. The incorporation of BFS and LS increased the thermal conductivity compared to mixtures containing only FS, indicating a higher heat transfer capacity. Although these substitutions modify the mortar's thermal behavior, the resulting increase in conductivity may limit their suitability for applications requiring enhanced thermal insulation.

Asadi et al. (2025) (Asadi *et al.*, 2025) investigated the incorporation of Micronal 24D, a microencapsulated phase change material (MPCM), added at a fixed proportion relative to cement

content in mortars. The inclusion of MPCM reduced both thermal conductivity and density, independent of cement dosage. These results indicate that MPCM effectively enhances the thermal insulation performance of mortars, contributing to improved energy efficiency without constraining cement composition.

Karakaş et al. (2023) (Karakaş *et al.*, 2023) examined the replacement of natural sand with expanded perlite (EP) and raw perlite (RP) in fly ash–based mortars. The mixture with EP as a full sand substitute showed markedly lower thermal conductivity and density compared to the RP-based mortar. These findings indicate that EP is more effective in improving thermal insulation and reducing unit weight, making it a preferable alternative for applications demanding enhanced thermal performance.

The study evaluates the thermal performance of different mortars applied as fire protection coatings for structural beams. Four beams (two reinforced concrete and two steel members with distinct cross-sectional geometries) were analyzed to assess temperature distribution within the cross section under fire exposure. A total of 23 mortar formulations with varying compositions and additives were considered. The objective is to identify the mortar types, mixture proportions, and additives that most effectively enhance structural thermal performance during fire.

2. MATERIALS AND METHODS

2.1 Mortar characteristics, parameters and nomenclatures

Table 1 summarizes the mortar formulations, including the reference mix (M1: cement, sand, and water) and 22 alternative mixtures incorporating partial or total replacements of cement, sand, or slag to enhance thermal performance. The modifications include fly ash and GFRP powder (M2–M6), raw vermiculite with CSA cement (M7–M8), phase change materials (M9–M10), recycled carbon black (M11–M12), olive solid waste (M13–M14), microencapsulated PCM (Micronal 24D) at 20% of cement weight (M15–M17), expanded and raw perlite as full sand replacements (M18–M19), vegetable synthetic sponge (M20–M21), and expanded PVC aggregates replacing a quarry/sea sand blend (M22–M23). Table 1 identifies each formulation and its literature source and where the thermal data was extracted to create the FEA model with the proposed mortar coatings..

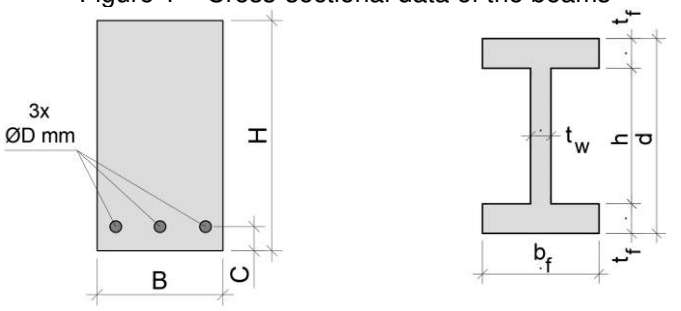
Table 1 – Mortar cases and nomenclatures

Mortar Name	Description	Reference
M1	Conventional mortar with cement and sand	Rong et al., 2024
M2	4% Glass Fiber Reinforced Polymers Powder and 16% Fly Ash cement replacement	
M3	4% Glass Fiber Reinforced Polymers Powder and 16% Fly Ash Slag replacement	
M4	40% Glass Fiber Reinforced Polymers Powder Slag replacement	
M5	40% Glass Fiber Reinforced Polymers Powder Cement replacement	
M6	40% Glass Fiber Reinforced Polymers Powder and 20% Fly Ash cement replacement	
M7	Raw Vermiculite 30% sand replacement	Kouadjo Tchekwagep et al., 2024
M8	Raw Vermiculite 100% sand replacement	
M9	Phase Change Material 20% sand replacement	Topçu et al., 2024
M10	Phase Change Material 40% sand replacement	
M11	Carbon Black 30% sand replacement	Zhao et al., 2023
M12	Carbon Black 100% sand replacement	
M13	Olive Solid Waste 5% sand replacement	EL boukhari et al., 2023
M14	Olive Solid Waste 15% sand replacement	
M15	Microencapsulated Phase Change Materials 20% cement weight addition	Asadi et al., 2025
M16	Microencapsulated Phase Change Materials 20% cement weight addition	
M17	Microencapsulated Phase Change Materials 20% cement weight addition	
M18	Expanded Perlite 100% Sand replacement	Karakaş et al., 2023
M19	Raw Perlite 100% Sand replacement	
M20	Vegetable Synthetic Sponge 5% sand replacement	Salem et al. 2020
M21	Vegetable Synthetic Sponge 20% sand replacement	
M22	lightweight aggregates of Expanded Polyvinyl Chloride 15% sand replacement	Latroch et al. 2018
M23	lightweight aggregates of Expanded Polyvinyl Chloride 75% sand replacement	

2.2 Beam cross-section geometries

A total of four cases of beams were tested: two for RC and two for steel. The difference between the two is the cross-section dimensions. The cross-section types are shown in Figure 1 and the geometric data in Table 2 and Table 3.

Figure 1 – Cross-sectional data of the beams



(a) Reinforced concrete beam (b) Steel beam

Table 2 – Reinforced concrete beams nomenclature

Beam name	B	H
Bc1	150 mm	500 mm
Bc2	250 mm	500 mm

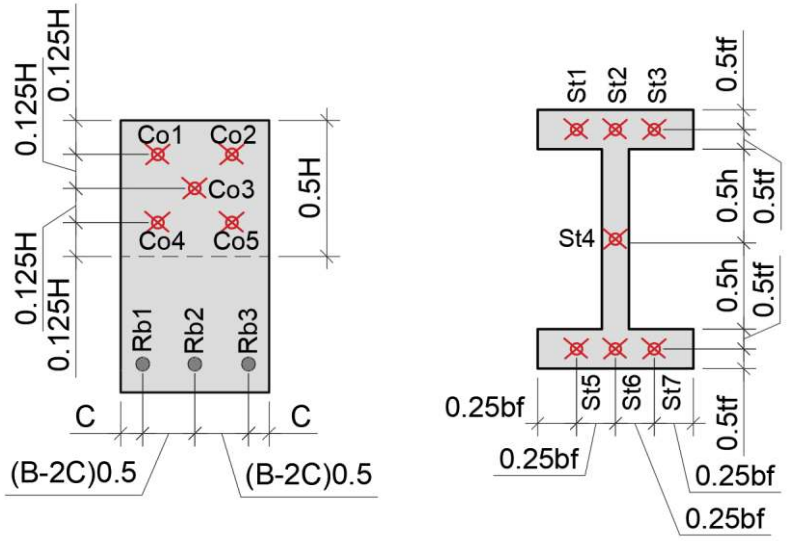
Table 3 – Steel beams nomenclature

Beam name	d	b_f	t_f	h	t_w
Bs1	229	210	23.7	180	14.5
Bs2	535	166	16.5	502	10.3

2.3 Control points

Fig.3 shown the control points assumed in the temperature measurements.

Figure 2 – Control points assumed in the average temperature of the beam cases



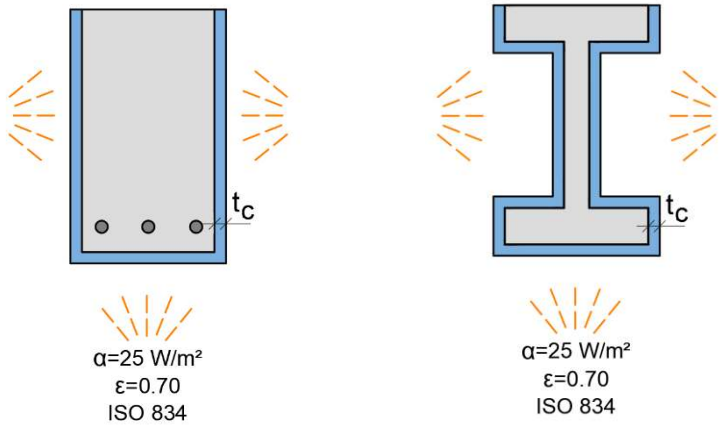
(a) Reinforced concrete beam (b) Steel beam

For the RC beams, temperatures were measured at locations relevant to analytical bending resistance calculations, namely in the concrete compression zone above the neutral axis and in the tensile reinforcement. The average concrete temperature was obtained from control points Co1 to Co5, and the average reinforcement temperature from Rb1 to Rb3 (Figure 3a). For the steel beams, the average temperature was calculated based on control points St1 to St7, as shown in Figure 3b.

2.4 FEA modelling

The temperature field in the cross-sections is governed by heat conduction, with thermal diffusivity defined as $\alpha=\lambda/(\rho\, Cp)$, where λ is thermal conductivity, ρ density, and Cp specific heat. Mortar properties were taken from Table 1, while the thermal parameters for concrete, reinforcement, and structural steel by Eurocode provisions. Convective and radiative heat transfer at the boundaries were defined considering convective and radiative data, ambient temperature (20 °C), and the fire temperature according to the ISO 834 (ISO 834-1, 2014). The problem was solved using a 3D nonlinear transient thermal model with DC3D8 solid elements and full integration. A refined mesh of 1.0 × 1.0 × 1.0 mm was adopted, with a temperature convergence tolerance of 0.1 °C and a time increment of 0.001 s.

Figure 3 – Heating process and parameters of the assumed beam cross-sections



(a) Reinforced concrete beam (b) Steel beam

The criteria and procedure for the FE model were validated by the authors through an extensive full-scale experimental test. Some of these results can be found in (Bolina, Poleto, *et al.*, 2023; Bolina, Schallenberger, *et al.*, 2023; Bolina and Rodrigues, 2023). The FEA numerical simulation is also based on the approaches presented by the authors in (Kodur and Phan, 2007).

3. RESULTS

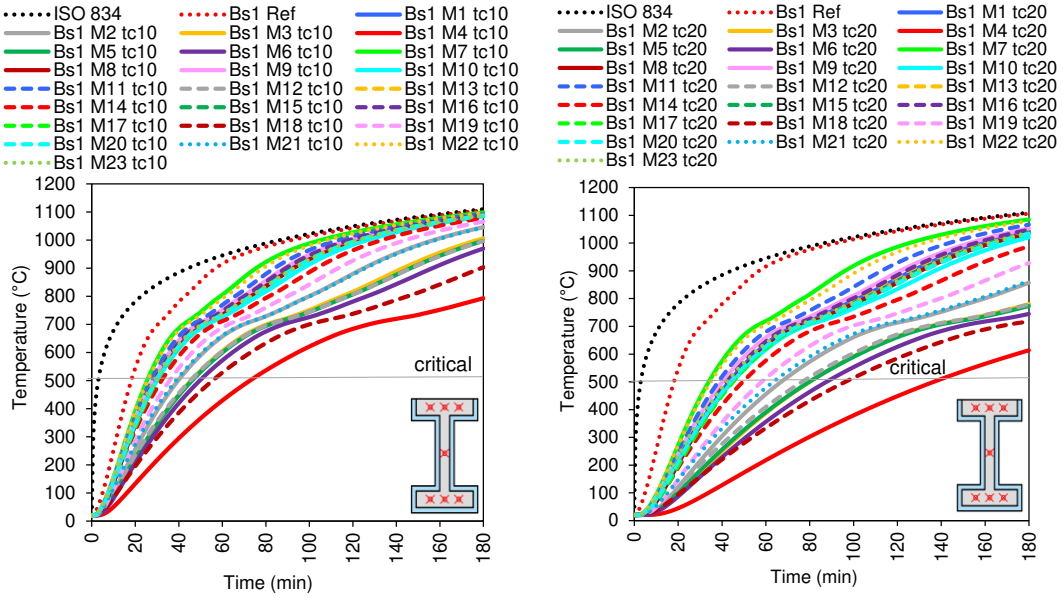
3.1 Bs1 beams

See Figure 5. Only M4 at 30 mm prevented the steel profile from reaching critical temperatures, confirming its superior performance. Thermal efficiency increased with thickness. For M4, reductions reached up to 95.0% (30 min, 30 mm), with maximum temperatures decreasing to 434.6 °C at 30 mm, below typical critical limits.

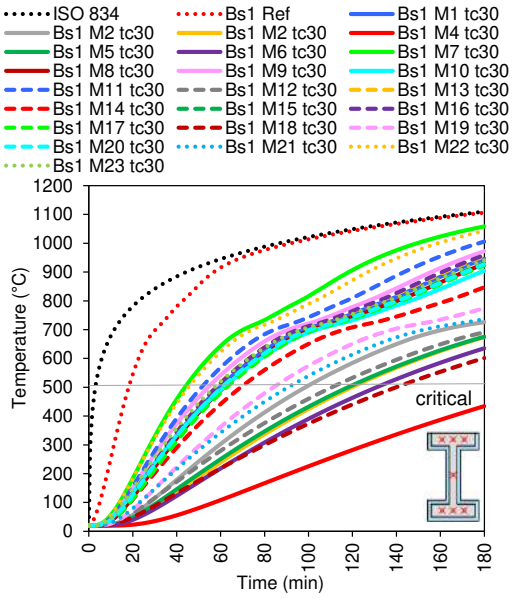
M18 (similar to M6) showed good early performance but decreasing efficiency over time; at 30 mm, reductions ranged from 87.4% (30 min) to 45.6% (180 min), with peak temperatures still

reaching 601.4 °C. M7 and M22 were the least effective. Even at 30 mm, reductions at 180 min were only 5.7%, and peak temperatures exceeded 1000 °C for all thicknesses, indicating limited suitability for structural fire protection.

Figure 4 – Cross-section temperature in the Bs1 beams



(a) c=10 mm (b) c=20 mm



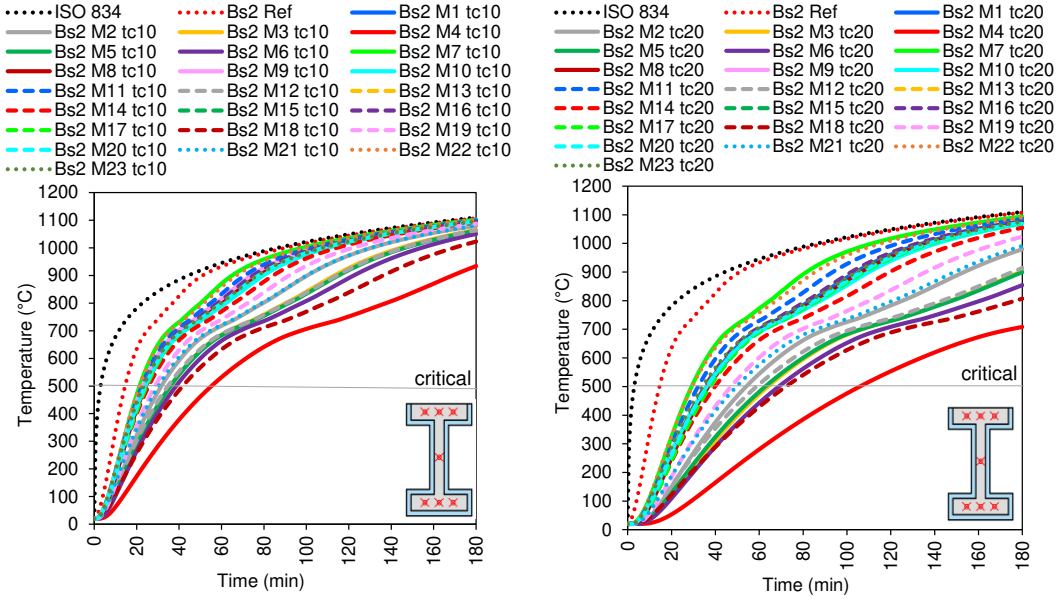
(c) c=30mm

3.2 Bs2 beams

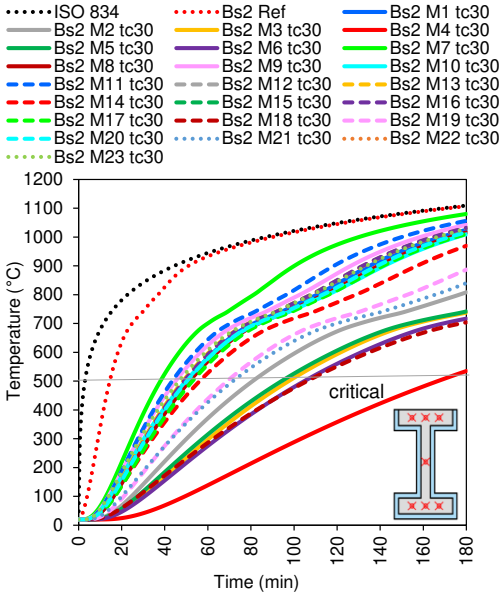
See Fig.6. None of the mortars prevented the steel profile from reaching the critical temperature, although M4 at 30 mm delayed this limit until 173 min, confirming its superior performance. The results also reflect the influence of the section factor (heated perimeter-to-area ratio), which governs heating rate but is beyond the present scope. M4 achieved the highest reductions, reaching 94.6% at 30 min (30 mm), with peak temperatures of 934.7 °C, 708.2 °C, and 534.9 °C for 10, 20, and 30 mm, respectively. M18 and M6 showed similar but slightly lower efficiency. In contrast,

M7 and M22 provided minimal long-term protection; even at 30 mm, reduction was only 3.0% at 180 min, with peak temperatures above 1070 °C. Overall, mortar type and thickness significantly affect steel heating, directly influencing mechanical degradation and fire resistance performance.

Figure 5 – Cross-section temperature in the Bs2 beams



(a) c=10 mm (b) c=20 mm



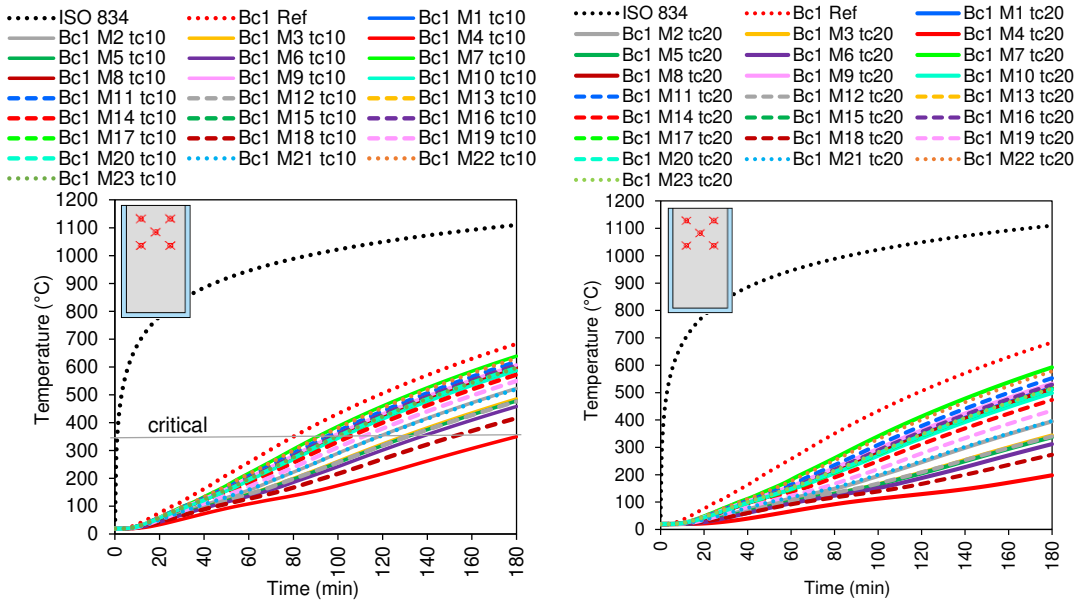
(c) c=30 mm

3.3 Bc1 beams

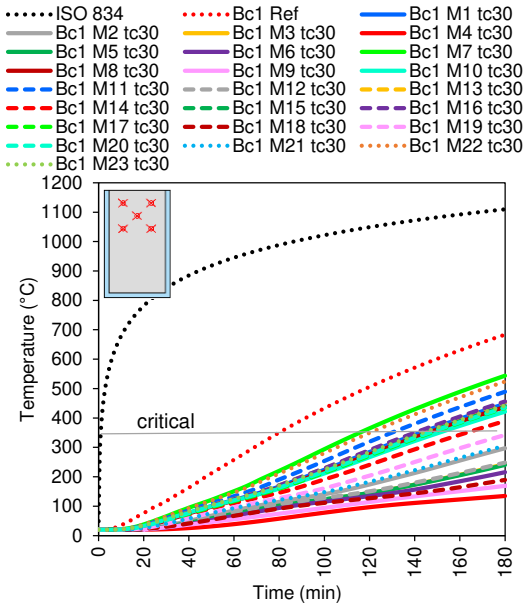
See Fig.7. A 10 mm mortar layer already provides meaningful protection against cross-sectional heating, though performance depends on composition. Mortars should therefore be considered in RC fire design. M4 showed the best results, reducing concrete temperatures by about 53–61% (10 mm), 71–75% (20 mm), and 80–84% (30 mm). Maximum temperature dropped from 683.2 °C (unprotected) to 349.9 °C, 198.2 °C, and 134.6 °C, respectively. M18 (similar to M6) offered good

but lower protection, while M7 and M22 were the least effective, with reductions below 16% at 10 mm and maximum temperatures still above 520 °C at 30 mm. In general, thickness and intrinsic thermal properties govern fire performance, affecting temperature rise and structural safety.

Figure 6 – Cross-section temperature in the concrete part in the case of Bc1 beams



(a) c=10 mm (b) c=20 mm



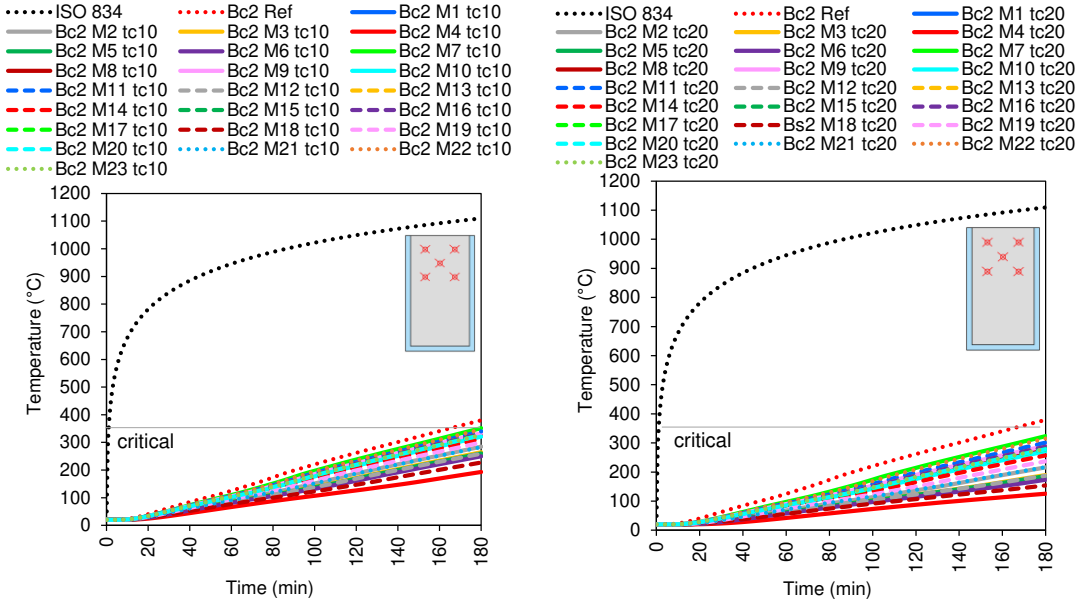
(c) c=30mmm

Reinforcement is the most temperature-sensitive component in RC members under fire. All mortars reduced rebar temperatures, with M4 and M18 showing the best performance. M4 limited maximum rebar temperatures to 577.1 °C (10 mm) and 228.2 °C (20 and 30 mm), with reductions reaching up to 91% during fire exposure. M18 also performed well, with maximum temperatures of 663.6 °C, 470.6 °C, and 344.4 °C for 10, 20, and 30 mm, respectively. In contrast, M7 and M22 were ineffective, with rebar temperatures remaining above 800 °C even at 30 mm thickness.

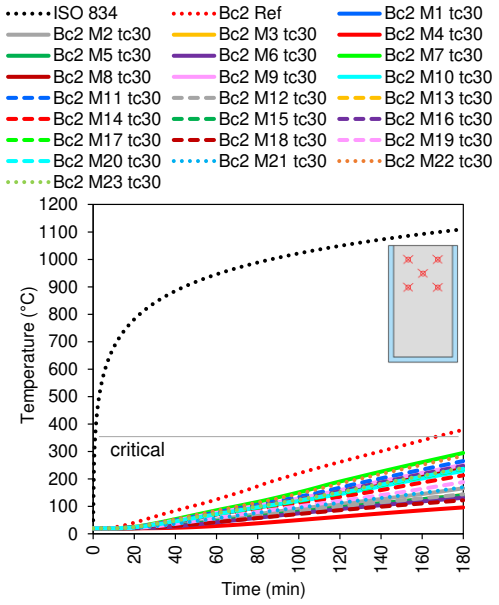
3.4 Bc2 beams

See Fig.9.

Figure 7 – Cross-section temperature in the concrete part in the case of Bc2 beams



(a) c=10 mm (b) c=20 mm



(c) c=30mmm

For beam Bc2, M4 again showed the best thermal performance. At 10 mm thickness, it reduced the average cross-sectional temperature by 70.7–75.2% during ISO 834 exposure; at 20 mm, reductions ranged from 79.9–83.0%, and at 30 mm reached up to 88.6% relative to the unprotected case. M18 presented the second-best performance, with reductions of 65.5–71.5% (10 mm), 75.0–78.5% (20 mm), and 79.8–83.6% (30 mm). M6 showed very similar behavior and can be considered thermally equivalent to M18. M7 and M22 exhibited the lowest performance, though still achieving average reductions of approximately 55%, 60%, and 65% for 10, 20, and 30 mm, respectively. Due to the beam's cross-sectional dimensions, concrete temperatures remained below

critical limits in all protected cases. Only the unprotected beam briefly reached critical levels, and with limited severity. Thus, for Bc2, mortar application is not essential for concrete protection but remains relevant for safeguarding reinforcement, as discussed subsequently.

Reinforcement temperature governs bending resistance and is therefore the critical parameter in RC fire design. While some mortars effectively prevent rebars from reaching critical temperatures, others provide limited protection, making mortar composition a decisive design criterion. M4 again showed the best performance and was the only mortar capable of preventing critical rebar temperatures at all thicknesses. At 10 mm, reductions ranged from 65.5% (30 min) to 40.9% (180 min); at 20 mm, from 83.2% to 63.8%; and at 30 mm, from 90.9% to 76.8%, demonstrating consistently high efficiency. M18 and M6 exhibited similar and moderate performance. For 10 mm, reductions decreased from about 56% (30 min) to 27% (180 min); for 20 mm, from 72% to 50%; and for 30 mm, from 84% to 63%, indicating reduced effectiveness with increasing fire duration. In contrast, M7 and M22 were the least effective and did not prevent critical temperatures. Even at 30 mm, reductions ranged only from 57% (30 min) to 17% (180 min). Overall, only M4 ensured adequate reinforcement protection across all thicknesses, confirming the importance of mortar type in structural fire design.

4. CONCLUSIONS

The study assessed 23 mortar formulations with different mixes and additives as thermal protection for steel and reinforced concrete members under fire. All mortars reduced internal temperatures, with performance governed by thickness and intrinsic thermal properties. The main conclusions are:

- Mortars incorporating GFRP as a slag substitute and expanded perlite as a sand replacement showed the highest thermal efficiency, achieving temperature reductions close to 100% in some cases.

- Mixtures containing 30% vermiculite or 15% expanded PVC exhibited the lowest performance, underscoring the importance of material selection.

- Additives such as GFRP powder and expanded perlite significantly improve insulation by reducing thermal conductivity; GFRP enhances thermal stability, while perlite increases porosity and thermal resistance.

- Further research is needed to optimize additive combinations and better understand their interaction effects.

- Specific heat was consistently absent in the reviewed experimental studies; future research should include its measurement to improve the accuracy of thermal analyses.

REFERENCES

Adediran, A., Yliniemi, J., Moukannaa, S., Ramteke, D.D., Perumal, P. and Illikainen, M. (2023), "Enhancing the thermal stability of alkali-activated Fe-rich fayalite slag-based mortars by

incorporating ladle and blast furnace slags: Physical, mechanical and structural changes", *Cement and Concrete Research*, Elsevier Ltd, Vol. 166, doi: 10.1016/j.cemconres.2023.107098.

Asadi, I., Ji, G., Steiner, G. and hajmohammadian baghban, M. (2025), "Impact of microencapsulated phase change materials (PCMs) on the thermal and mechanical performance of cement mortar", *Developments in the Built Environment*, Elsevier Ltd, Vol. 21, doi: 10.1016/j.dibe.2024.100594.

Bolina, F.L., Poleto, G. and Carvalho, H. (2023), "Proposition of parametric data for UHPC at high temperatures", *Journal of Building Engineering*, Vol. 76, p. 107222, doi: https://doi.org/10.1016/j.jobe.2023.107222.

Bolina, F.L. and Rodrigues, J.P.C. (2023), "Finite element analysis criteria for composite steel decking concrete slabs subjected to fire", *Fire Safety Journal*, Vol. 139, p. 103818, doi: https://doi.org/10.1016/j.firesaf.2023.103818.

Bolina, F.L., Schallenberger, M. and Carvalho, H. (2023), "Experimental and numerical evaluation of RC ribbed slabs in fire conditions", *Structures*, Vol. 51, pp. 747–759, doi: https://doi.org/10.1016/j.istruc.2023.03.057.

EL boukhari, M., Merroun, O., Maalouf, C., Bogard, F. and Kissi, B. (2023), "Enhancing mechanical and thermal properties of sustainable cement mortar through incorporation of olive solid waste aggregates", *Materials Today: Proceedings*, Elsevier BV, doi: 10.1016/j.matpr.2023.09.007.

ISO 834-1. (2014), "Fire-resistance tests - Elements of building construction - Part 1: General requirements", International Organization for Standardization (ISO), Geneve, Switzerland.

Karakaş, H., İlkentapar, S., Durak, U., Örklemez, E., Özuzun, S., Karahan, O. and Atiş, C.D. (2023), "Properties of fly ash-based lightweight-geopolymer mortars containing perlite aggregates: Mechanical, microstructure, and thermal conductivity coefficient", *Construction and Building Materials*, Elsevier Ltd, Vol. 362, doi: 10.1016/j.conbuildmat.2022.129717.

Kodur, V.K.R. and Phan, L. (2007), "Critical factors governing the fire performance of high strength concrete systems", *Fire Safety Journal*, Vol. 42 No. 6–7, pp. 482–488, doi: 10.1016/j.firesaf.2006.10.006.

Rong, X., Xu, W., Zhang, T. and Zhang, J. (2024), "Mechanical and thermal properties of insulated mortar incorporated with GFRP powder", *Construction and Building Materials*, Elsevier Ltd, Vol. 416, doi: 10.1016/j.conbuildmat.2024.135259.

Topçu, İ.B., Bayram, M., Ustaoğlu, A., Hekimoğlu, G., Erdoğmuş, E., Sarı, A., Gencel, O., *et al.* (2024), "Innovative cementitious mortar incorporated with sepiolite based shape-stable phase change material for thermal controlling of buildings", *Construction and Building Materials*, Elsevier Ltd, Vol. 426, doi: 10.1016/j.conbuildmat.2024.136124.

Zhao, J., Huang, G., Guo, Y., Gupta, R. and Liu, W.V. (2023), "Developing thermal insulation cement-based mortars using recycled carbon black derived from scrapped off-the-road tires", *Construction and Building Materials*, Elsevier Ltd, Vol. 393, doi: 10.1016/j.conbuildmat.2023.132043.